




Clinically relevant biomechanical properties of three different fixation techniques of the upper instrumented vertebra in deformity surgery

Edin Nevzati¹ · Manuel Moser¹ · Nick Dietz² · Burt Yaszay³ · Lawrence G. Lenke⁴ · Mazda Farshad⁵ · Varun Arvind⁶ · Samuel K. Cho⁶ · Alexander Spiessberger⁷ 

Received: 26 December 2021 / Accepted: 26 March 2022 / Published online: 15 April 2022
© The Author(s), under exclusive licence to Scoliosis Research Society 2022

Abstract

Objective Adjacent segment disease, junctional kyphosis/failure and pseudarthrosis can negatively impact the mid to long-term outcome in spinal deformity surgery. These complications might be influenced by upper instrumented vertebra (UIV) fixation techniques. In this study we analyze key biomechanical properties of three different UIV fixation techniques and define their ideal clinical use based on patient-specific risk profiles using a finite element analysis (FEA) model.

Methods A T9–pelvis posterior instrumented spinal fusion was assumed. Three different FEA models were created based on the UIV fixation technique: T9 pedicle screws (PS); T9 cortical bone screws (CBS); T9 transverse process hooks (TPH). The three FEA models consisted of T8–T10 bone and ligamentous anatomy derived from a CT scan of a healthy patient as well as spinal implants consisting of either pedicle screws, cortical bone screws or transverse process hooks as well as cobalt chromium rods. The FEA models were constrained at T10, axial load as assumed for a healthy 80 kg male during flexion, extension and lateral bending were applied. As surrogate markers for risk of proximal junctional kyphosis, proximal junctional failure, adjacent segment disease and pseudarthrosis the following biomechanical parameters were calculated: UIV range of motion (ROM); intradiscal stress at UIV/UIV + 1; UIV intravertebral stress and screw pull out forces. One-way ANOVA analyses have been performed to compare biomechanical outcome parameters between the three construct variants under investigation.

Results UIV-ROM was restricted during flexion/extension/lateral bending by: PS: 73%/80%/86%, CBS: 71%/81%/85% and TPH: 62%/76%/85%. Average intradiscal stress at UIV/UIV + 1 during flexion/extension/lateral bending was (Mega Pascal, MPa): PS 0.42/0.44/0.38, CBS 0.49/0.4/0.44, TPH 0.66/0.51/0.58; average intravertebral stress of the UIV superior endplate during flexion/extension/lateral bending was (MPa): PS 2.23/2.12/2.21, CBS 1.87/1.98/1.8, TPH 1.67/0.98/1.53. Screw pull-out forces (N) at UIV during flexion/extension/lateral bending were: PS 476/320/375, CBS 444/245/308. Statistically significant differences were found for intradiscal stress as well as vertebral body average stress ($p=0.02$ and $p=0.02$).

Conclusion Different UIV fixation techniques carry different biomechanical properties. Pedicle screw fixation is the most rigid, leading to the highest UIV stress and UIV screw pull out forces. Cortical bones screw fixation is similarly rigid; however, UIV stress and UIV screw pull out is significantly lower. Transverse process hook fixation is the least rigid, with the lowest UIV stress, however highest intradiscal stress at UIV/UIV + 1. Thus, these biomechanical differences may help select optimal UIV fixation techniques according to patient specific risk factors.

Keywords Junctional kyphosis · Junctional failure · Cortical bone screw · FEA

Introduction

Mid and long-term outcomes following spinal deformity surgery can be negatively influenced by possible secondary alterations at the transition between fused and unfused spine. These secondary changes are on a clinical spectrum ranging from more benign degenerative changes of discs and facet joints, termed adjacent segment disease (ASD) to

✉ Alexander Spiessberger
alexander.s.spiessberger@gmail.com

Extended author information available on the last page of the article

structural failure patterns in terms of junctional kyphosis (JK) or junctional failure (JF). A variety of patient specific factors are known to influence the incidence of JK and JF, mainly bone quality, patient age and body weight [1, 2]. Further surgery-specific factors such as length of fusion, choice of upper and lower instrumented vertebra (UIV and LIV) and postoperative alignment influence the incidence of JK/JF [3]. Previous clinical research suggests that less rigid UIV-fixation, such as transverse process hooks (TPH) might decrease the risk of JK/JF in patients who are not at high risk for pseudarthrosis [4]. Lately another fixation technique has been introduced in the lumbar spine, the so-called cortical bone screw (CBS) trajectory, which comprises of an upward and outwardly direct pedicle screw. This technique requires less soft tissue dissection to expose the entry point and engages more of the corresponding lamina, which is rich in dense cortical bone. The choice of UIV fixation technique has a profound impact on the biomechanical characteristics of the junctional area with resulting clinical implications.

This study investigates the properties of three different UIV fixation devices: conventional pedicle screw fixation (PS), CBS and TPH. CBS is a novel technique which we compare to the two established techniques, PS and TPH. The biomechanical profile of each device is correlated with possible clinical correlations to facilitate surgical decision making.

Methods

The CT scan of a 20-year-old male without pathologic structural changes of the entire spine and no known disease of bone metabolism was used as a template for this study. Thin

sectioned (0.625 mm) DICOM files were used to extract the spinal segment T8–T10 and then converted to a “computer-aided design” (CAD) model, which then was used for the FEA Simulation[5]. Three different surgical scenarios have been modelled, differing by the mode of UIV fixation: variant 1: UIV, UIV-1 PS, variant 2: UIV CBS and UIV-1 PS, variant 3 UIV TPH and UIV-1 PS; Virtual placement of hardware was performed using 3D surface rendered views in correlation with cross sectional views according to common surgical practice [6–8], see Fig. 1.

Pedicle screws as well as TPH were titanium based and dimensions chosen according to local anatomy, while rods were cobalt chromium based [9].

Each vertebra consisted of a cancellous core model using 3D tetra element surrounded by a cortical shell which is modelled using 2D elements. The intervertebral disc was modelled as nucleus pulposus and annulus fibrosus as a hyper-elastic material using the Mooney–Rivlin material model [10]. Facet joints of each level were modeled as a tetra element and major ligaments (anterior longitudinal ligament, ALL, interspinous ligament, ISL and supraspinous ligament, SSL) as shell elements [11]. Figure 2 outlines biomechanical material properties of all simulated implant and anatomical elements.

Pedicle screw placement was performed on the 3D models using a conventional trajectory, as described in the literature [7, 12]. Cortical bone screw placement has been performed as described by Hosogane et al. [8]. Friction coefficient between the bone and the pedicle screw has been considered according to previous studies [13].

Considering an estimated total body weight of 75 kg, in which 65% constitutes to upper body weight, a load of 480 Newton (N) was applied on the FEA models vertically.

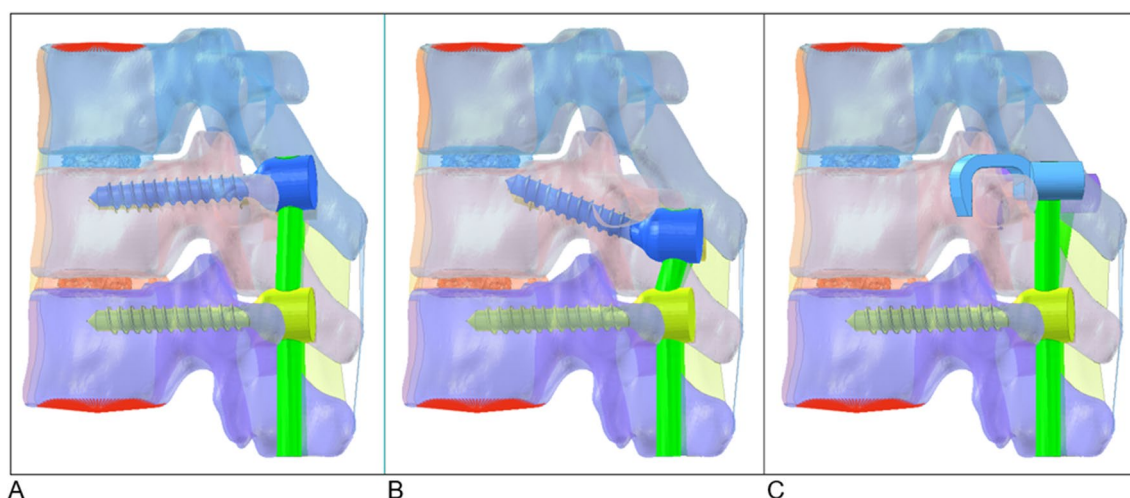


Fig. 1 A T9-pelvis PSF scenario has been assumed. Three different UIV (T9) fixation techniques have been simulated in separate FEA models: **A:** variant 1, classical pedicle screw (CBS) fixation, **B:** vari-

ant 2, cortical bone screw (CBS) trajectory, **C:** variant 3, transverse process (TP) hook fixation

Material	Parts	Density (g/cm ³)	E (MPa)	Poisson's ratio	Cross-Section (mm ²)/ Width from model (mm)/ Thickness considered (mm)
linear	Cancellous bone	1.87	100	0.2	
Linear (2D Shell Elements)	Cortical shell	1.91	12000	0.3	0.31 mm (thickness)
Linear (2D Shell Elements)	Cartilaginous endplate	1.003	23.8	0.4	0.8 mm (thickness)
Linear	Bony end plate		12000	0.3	-
Hyper elastic	Nucleus pulposus	1.003	C1=0.12, C2=0.03	0.499	-
Hyper elastic	Annulus fibrosus	1.003	C1=0.18, C2=0.045	0.45	-
Chromium cobalt	Rod	10	210,000	0.29	-
Titanium	Screw	4.5	116,000	0.34	-
Linear (2D Shell Elements)	Interspinous Ligaments (ISL)		8	0.3	14.1/21.5/0.65
Linear (2D Shell Elements)	Supraspinous Ligaments (SSL)		8	0.3	10.5/2.6/4
Linear (2D Shell Elements)	Anterior Longitudinal ligaments (ALL)		7.8	0.3	22.4/20/1.12
linear	Facet Capsulary Ligaments (FCL)		7.5	0.3	-

Fig. 2 In each FEA model the spinal segments T8–T10 have been modelled using the above outlined material characteristics

Moments required for flexion, extension and lateral bending were derived using an intact model based on the maximum range of motion (ROM) of T9, which was then applied to the instrumented FEA models. All degrees of freedom were constrained at the T10 endplate. Each FEA model of the corresponding variant under investigation has been subjected to flexion, extension and lateral bending loads. During each simulation the following parameters have been calculated: ROM T9, intradiscal von Mises stress UIV/UIV + 1, intra-vertebral von Mises stress UIV, implant associated von Mises stress, screw pull out force.

Biomechanical outcome parameters were compared between the three variant models using one-way ANOVA analysis (Graphpad Software, La Jolla, San Diego, USA).

Results

Rigidity of a fixation technique was investigated by comparing the UIV-ROM of each variant to a native, intact FEA model of T8–T10. Table 1 outlines ROM restrictions under the above outlined loading conditions, showing that TPH-variant, particularly during flexion, allowed for the most residual movement when compared to the other two variants.

PS and CBS variants showed comparable reduction in UIV-ROM in relation to the TPH-variant of 81%, 83% and 89% and 76%, 80%, and 98% (flexion, extension, and lateral bending) for PS and CBS, respectively.

Intradiscal pressures at UIV + 1/UIV (measured in mega Pascal, MPa) were calculated after loading conditions were applied and are outlined in Table 1. Figure 3 shows mid

discal axial sections (UIV/UIV + 1) demonstrating von Mises stress zones for each variant, while Table 1 shows average von Mises stress values calculated for a single mid disc axial section. While PS and CBS resulted in comparable mean stress values (relative values for PS and CBS during flexion/extension/lateral bending: 100%/100%/86% and 117%/91%/100%), TPH showed significantly higher stresses 157%/116%/131%).

Intravertebral von Mises stress at the UIV under loading conditions are illustrated in Figs. 4 and 5. In each FEA simulation the UIV was divided into a superior and inferior half in a sagittal plane. Average von Mises stress values under loading conditions are detailed in Table 1. Except for extension loading in variant 3, average stresses were higher in the superior half of the vertebral body for all variants. Upon flexion the highest average stress was encountered in the PS variant (2.23 MPa versus 1.87 and 1.67 MPa, for PS, CBS and TPH, respectively). The PS variant also had the highest average stress in extension (2.12 MPa versus 1.98 and 0.98 MPa, respectively) and in lateral bending (2.21 MPa versus 1.8 MPa versus 1.53 MPa). Table 1 also outlines maximal von Mises stress values for each variant and loading condition. Correlating these results with Fig. 4 show that the engagement site of the TPH are high stress areas (5.06 MPa, 5.41 MPa, and 5.72 MPa during flexion, extension and lateral bending, respectively). Moreover, the cortical area directly caudal to the entry point of the cortical bone screw trajectory is subject to higher stresses (flexion, extension and lateral bending: 3.29 MPa, 2.68 MPa and 2.95 MPa respectively). Actual implant related stresses are outlined in Fig. 6,

Table 1 Biomechanical measurements

	Variant 1 (pedicle screw)	Variant 2 (cortical bone screw trajectory)	Variant 3 (transverse process hook trajectory)
UIV fixation	Pedicle screw, classic trajectory	Pedicle screw, cortical bone screw trajectory	Transverse process hook
Range of motion (ROM), °			
Flexion	0.6 (81%)	0.64 (76%)	0.84 (100%)
Extension	0.3 (83%)	0.29 (80%)	0.36 (100%)
Lateral bending	0.43 (93%)	0.45 (98%)	0.46 (100%)
Intradiscal average stress (von Miess), UIV/UIV + 1, MPa			
Flexion	0.42 (100%)	0.49 (117%)	0.66 (157%)
Extension	0.44 (100%)	0.4 (91%)	0.51 (116%)
Lateral bending	0.38 (86%)	0.44 (100%)	0.58 (131%)
Vertebral average stress (von Miess, MPa), superior half of UIV			
Flexion	2.23 (100%)	1.87 (84%)	1.67 (75%)
Extension	2.12 (100%)	1.98 (93%)	0.98 (46%)
Lateral bending	2.21 (100%)	1.8 (81%)	1.53 (69%)
Vertebral average stress (von Miess, MPa), inferior half of UIV			
Flexion	1.4 (100%)	1.28 (91%)	1.29 (92%)
Extension	1.73 (91%)	1.91 (100%)	1.28 (67%)
Lateral bending	1.44 (100%)	1.4 (97%)	1.1 (76%)
Vertebral maximum stress (von Miess, MPa), UIV			
Flexion	2.54 (51%)	3.29 (65%)	5.06 (100%)
Extension	1.95 (36%)	2.68 (49%)	5.41 (100%)
Lateral bending	2.02 (35%)	2.95 (52%)	5.72 (100%)
Implant maximum stress (von Miess, MPa)			
Flexion	131.5 (84%)	129.2 (82%)	157.7 (100%)
Extension	101.1 (64%)	129.8 (82%)	157.8 (100%)
Lateral bending	106.6 (75%)	142.9 (100%)	114.5 (80%)
Screw pull out forces (von Miess, N), UIV			
Flexion	476.3 (100%)	443.8 (93%)	–
Extension	319.8 (100%)	244.8 (77%)	–
Lateral bending	374.7 (100%)	308.0 (82%)	–

showing that high stress zones are located at the UIV screw head/ shaft interface in case of PS and CBS variants, particularly upon flexion. In the case of CBS, an additional high stress zone is located in the rods between UIV and UIV-1 and in the TPH variant high stress zones are located in the actual transverse process hooks (Table 1). Lastly screw pull out forces were calculated for each variant upon loading with PS having greater pull out forces in flexion, extension, and lateral bending when compared to CBS (Table 1). A statistical comparison of outcome parameter has been performed and is outlined in Fig. 7 and Table 2. Statistical significance was found for vertebral body stress values (MPa) as well as intradiscal stress (MPa). For the remaining parameters the sample size in terms of measurements has not been sufficient.

Discussion

The results of this biomechanical study indicate that the three different UIV fixation techniques (PS, CBS, TPH) have different biomechanical properties, potentially translating to a different risk profile for pseudarthrosis rate, ASD, and JK/JF. We find that while PS induces high UIV stress, it also is the most rigid mode of fixation. CBS is similarly rigid as PS, however UIV stress as well as screw pull out forces are lower when compared to CPS. TPH fixation showed the least rigid fixation, the lowest UIV stress however UIV/UIV + 1 intradiscal stress was highest. In a clinical setting the choice of UIV fixation technique based on these biomechanical results should be influenced by patient specific factors.

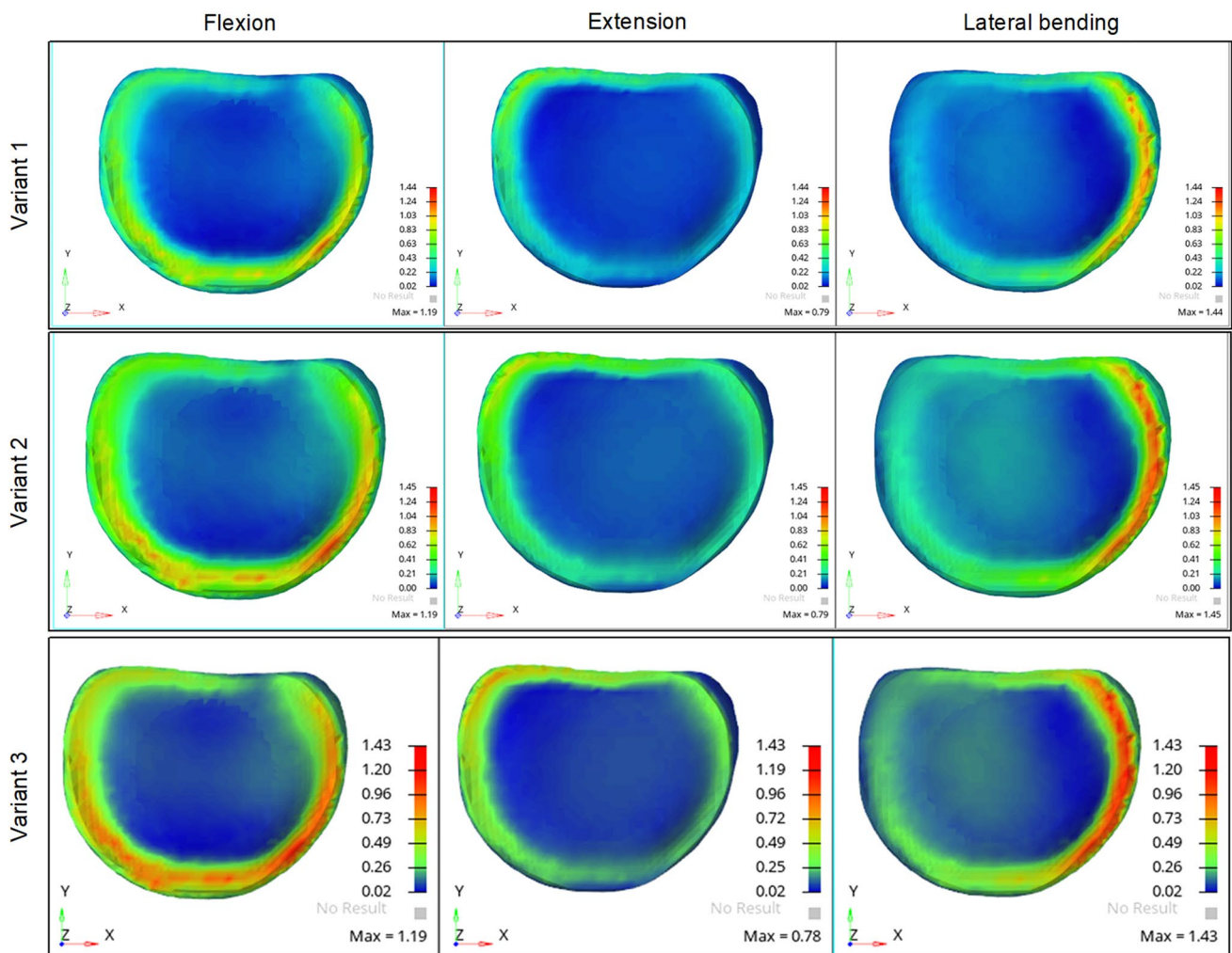


Fig. 3 Intradiscal von Mises stress (mega Pascal, MPa) at UIV/UIV + 1. Calculations were obtained in an axial plane at the mid-level of the disc space

Different approaches have been proposed in the past to improve the biomechanical profile at the junctional area of a fusion, such as polyester or mersilene tethering. As shown by Bess et al. [14] posterior polyester tethers at UIV to UIV + 1,2,3 create a gradual increase in ROM at the junctional zone as well as decrease of intradiscal pressures. In clinical trials junctional tethering has shown promising results with lower rates of PJF of 4% versus 18% [15, 16].

Pseudarthrosis following adult deformity surgery negatively impacts patient outcomes and has been reported in up to 24% of cases, with the thoracolumbar and lumbosacral junction being at highest risk [17]. Generally, risk factors for pseudarthrosis are advanced age, incomplete sacropelvic fixation (LIV S1 versus pelvis), residual postoperative global imbalance, thoracolumbar kyphosis ($> 20^\circ$) and osteoarthritis of the hip joint. In this study, we demonstrated, that ROM restriction, which can potentially influence fusion rate, was highest for the PS and CBS-variant when compared to TPH

fixation. In cadaveric studies it has been shown that in the native spine ROM at T1/2 is almost 50% higher than that of any other thoracic level [18]. Overall UIV-TP hook fixation may increase risk for pseudarthrosis, particularly if T2 is the UIV.

Initially JK has been defined as sagittal Cobb angle UIV/ UIV + 2 of more than 10° plus an increase between pre- and postop of at least 10° [19]. More recently, a novel definition of at least 15° increase between pre- and postop, measured between UIV and UIV + 1 [20] has been suggested. Mechanisms implicated in JK involve chronic endplate fractures of the UIV [21] in the lower thoracic spine and sUBLuxation in the upper thoracic spine case of proximal thoracic UIV [22]. The observations of our study support these results, since the upper half of the UIV represents the highest stress zone. Instrument related factors have been suggested to increase risk of JK include pedicle versus transverse process hook fixation, rod diameter (transitional rod), sagittal rod

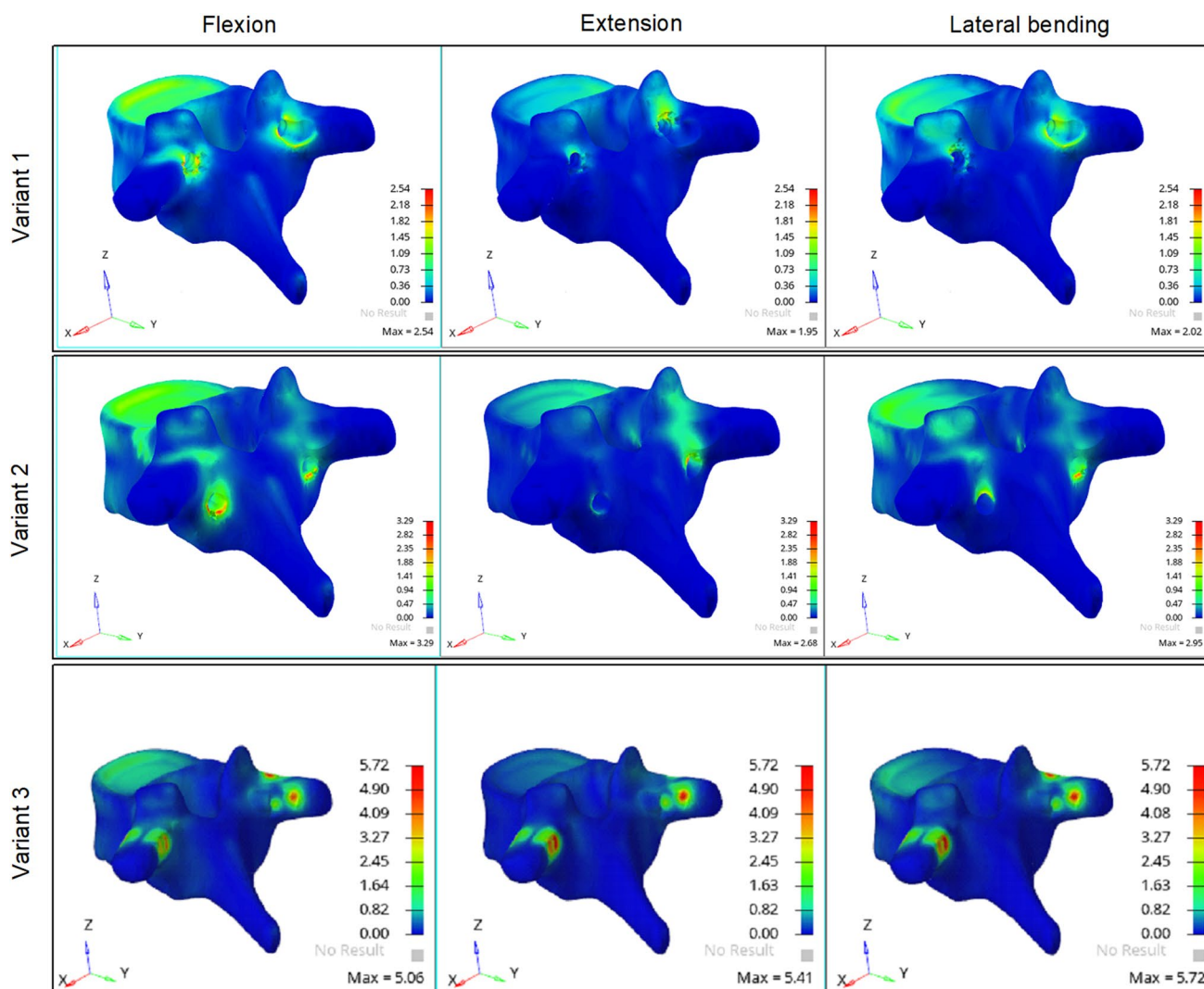


Fig. 4 UIV intravertebral von Mises stress (mega Pascal, MPa)

bend, and intraoperative violation of UIV facet joints [23]. Previous studies have found the incidence of JK in adults following deformity correction to be at 22%, even though outcome measures seem to not be impacted. Eventually only 11% of all PJF patients required revision surgery. Surgery related risk factors are posterior fusion (in contrast to anterior fusion), fusion to the sacrum, postoperative under- or overcorrection, total amount of alignment change [24], while patient specific risk factors include obesity [25]. In the case of JF, which manifests more seriously, in addition to UIV fracture, usually hardware failure is implicated as well. The incidence of JF has been found to be as high as 35%, with a revision rate of 21% [26] and risk factors include lower thoracic spine instrumentation and overcorrection. In this study we showed that TPH fixation led to the lowest UIV intravertebral stresses, which might decrease the risk for endplate fractures, related to JF. Clinical studies on the

utility of transverse process hooks came to varying conclusions. In a series of 39 adult patients, undergoing deformity correction, Matsumara et al. [4] found similar JK rates in patients with UIV-PS and TPH fixation, however the rate of JF was lower in patients with TPH fixation. In another study on 53 adult patients a significantly higher JK rate was found in patients with UIV-TPH fixation when compared to UIV-PS (36% vs 8%) [21].

As outlined in Table 1 the downsides of TPH are increased UIV/UIV + 1 intradiscal stress and lower rigidity of fixation. CBS, which demonstrate similar rigidity when compared to PS, induced less UIV endplate stresses and screw pull out, both of which are implicated in JF. Biomechanically it seems, that CBS might be a potential alternative to CPS fixation, however clinical experience with this trajectory in the thoracic spine is limited. Moreover, the entry point of CBS are not in line with CPS. Because of the upward/outward directed trajectory of

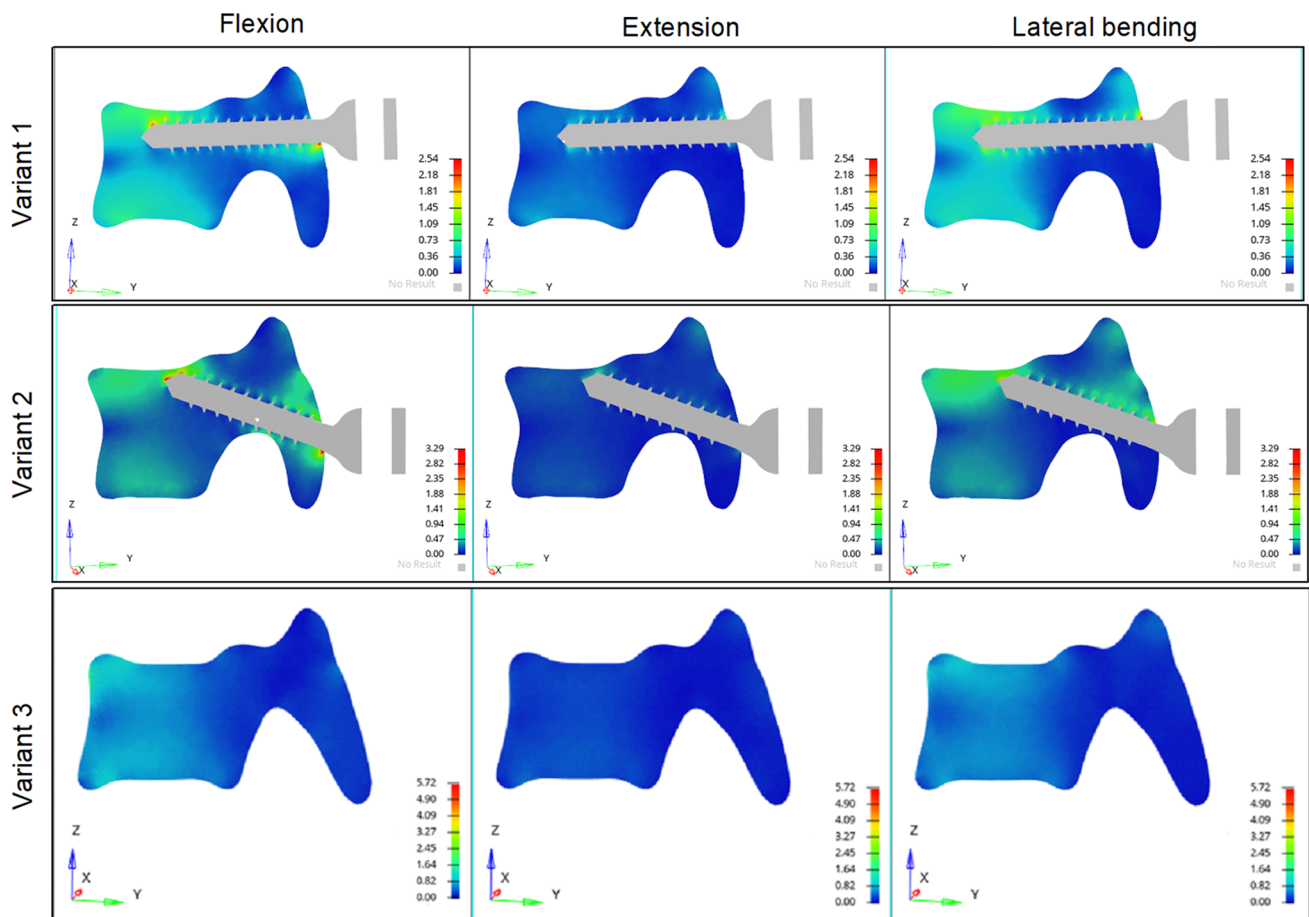


Fig. 5 UIV intervertebral von Mises stress (mega Pascal, MPa) in a single sagittal plane

CBS, less soft tissue damage might be necessary at the UIV/UIV + 1 junctional area in clinical practice, further decreasing the risk for JK/JF. As shown in this study the rods between UIV/UIV-1 is at particular stress in the case of cortical bone screw fixation, since the entry point for this trajectory is not in line with the entry point of classical pedicles screws. In clinical practice this fact would need to be addressed, for instance by appropriate rod contouring or the use of offset connectors.

Classical ASD is a significant burden in the lumbar spine. Even though less prevalent in the thoracic spine, due to its increased rigidity and decreased discal ROM, it should also be considered in certain scenarios. As this study showed, TP hook fixation leads to the highest discal stresses at UIV/UIV + 1, which could have implications in the case of pre-existing discal degeneration or congenital spinal stenosis.

Conclusion

The choice of UIV fixation technique (PS, CBS or TPH) has profound biomechanical implications, with instrumentation choice depending on individual patient risk profiles. PS and CBS are equally rigid modes of fixation; however, CBS induces less intravertebral stresses and less screw pull out forces thus potentially reducing the risk for JF. Our results suggest that TPH fixation might have the lowest risk for JF, however the risk for pseudarthrosis and adjacent segment disc degeneration might be high. The use of TPH might be less beneficial in cases with preexisting discal degeneration or congenital spinal stenosis at UIV/UIV + 1 or in cases with increased risk for pseudarthrosis.

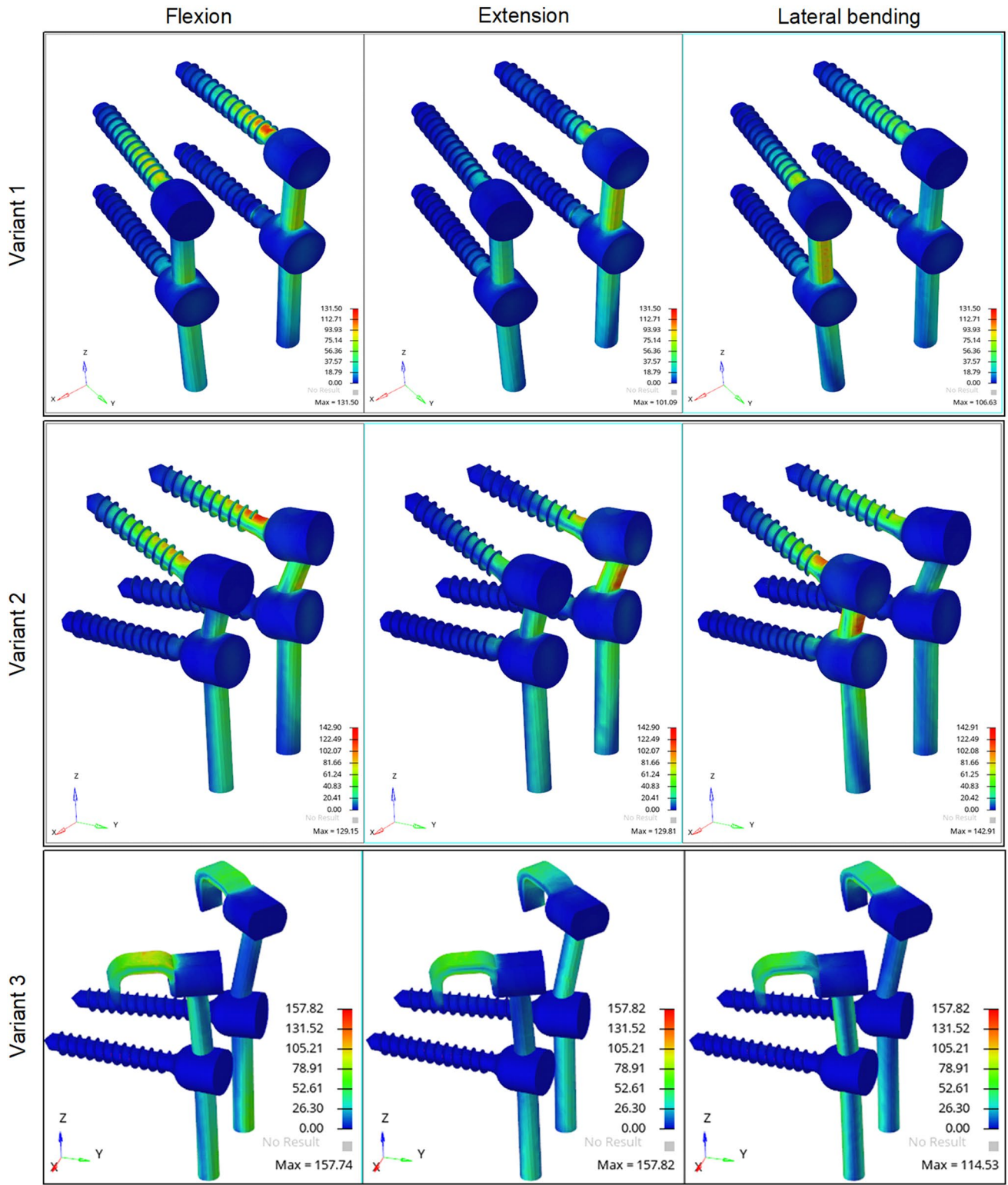


Fig. 6 Maximum implant related von Mises stress (mega Pascal, MPa)

Fig. 7 Statistical comparison of outcome parameters between three variant models: **A:** range of motion UIV/UIV + 1, **B:** intradiscal average stress (MPa, UIV/UIV + 1), **C:** vertebral body average stress (MPa, UIV), **D:** implant related maximum stress (MPa), **E:** screw pull out forces (N)

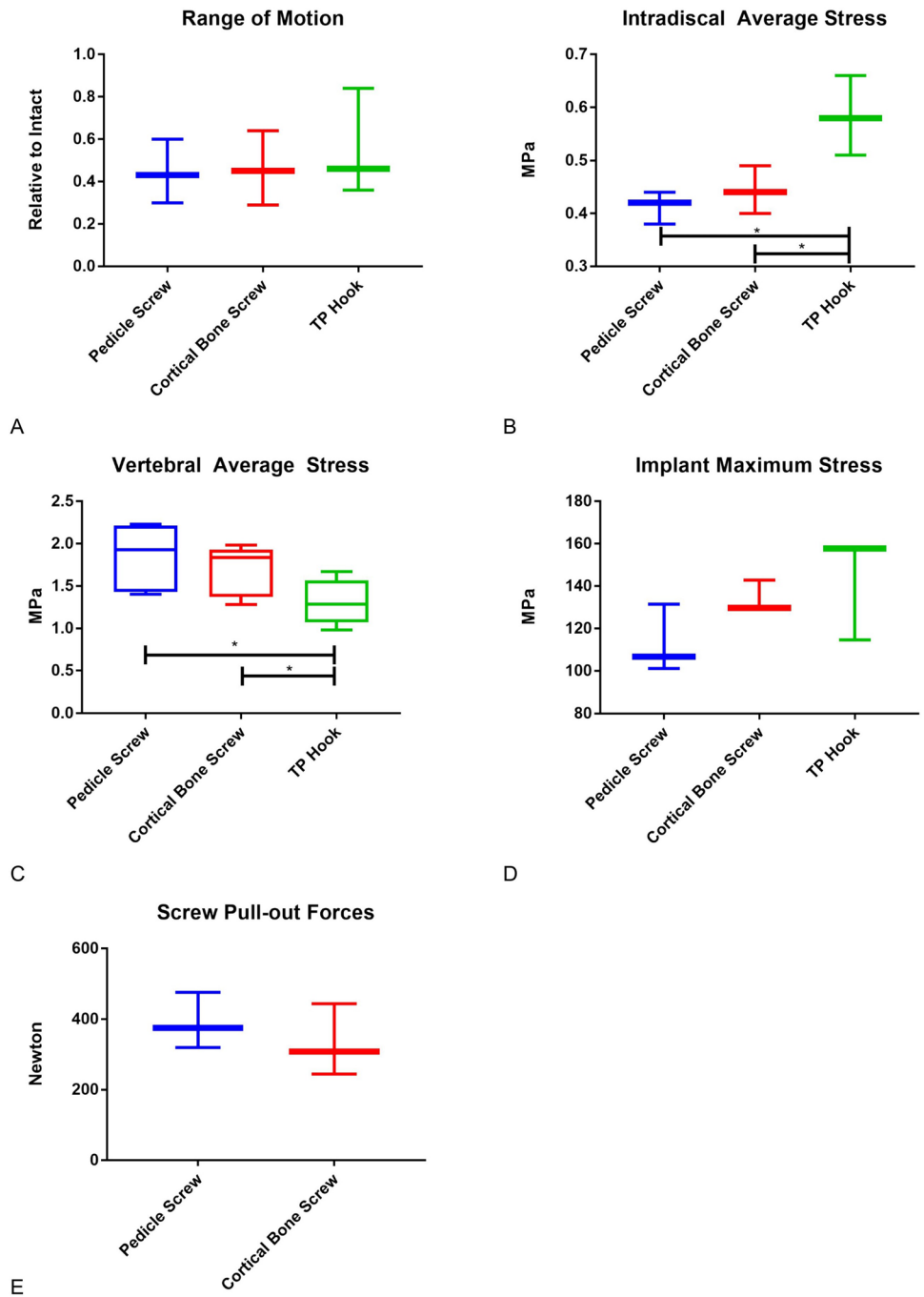


Table 2 Statistical comparison of biomechanical outcome parameters using one-way ANOVA

	ANOVA	Significance
Range of motion (°)	$F(2, 6) = 0.2693$	$P = 0.7727$
Intradiscal average stress (MPa)	$F(2, 6) = 8.616$	$P = 0.0172$
Vertebral average stress (MPa)	$F(2, 15) = 4.822$	$P = 0.0241$
Implant maximum stress (MPa)	$F(2, 6) = 2.28$	$P = 0.1834$
Screw pull-out forces (Newton)	$F(2, 2) = 1.64$	$P = 0.7576$

Author contributions EN, MM, ND, BY, LGL, MF, VA, SKC: conception, drafting, data analysis, manuscript preparation. AS: conception, drafting (original draft and final approval), data collection, manuscript preparation.

Funding Funding for this study was received by EN and MM from Medtronic.

Declarations

Ethical approval Approval by IRB and informed consent were not required for this study.

Conflict of interest None of the authors have a conflict of interest to declare.


References

- Wang H, Ma L, Yang D et al (2017) Incidence and risk factors of adjacent segment disease following posterior decompression and instrumented fusion for degenerative lumbar disorders. *Medicine* 96:e6032
- Liu F-Y, Wang T, Yang S-D et al (2016) Incidence and risk factors for proximal junctional kyphosis: a meta-analysis. *Eur Spine J* 25:2376–2383
- Kim JS, Phan K, Cheung ZB et al (2019) Surgical, radiographic, and patient-related risk factors for proximal junctional kyphosis: a meta-analysis. *Global Spine J* 9:32–40
- Matsumura A, Namikawa T, Kato M et al (2018) Effect of different types of upper instrumented vertebrae instruments on proximal junctional kyphosis following adult spinal deformity surgery: pedicle screw versus transverse process hook. *Asian Spine J* 12:622
- Wang T, Cai Z, Zhao Y et al. Development of a three-dimensional finite element model of thoracolumbar kyphotic deformity following vertebral column decancellation. *Applied bionics and biomechanics* 2019; 2019:
- Xuan J, Chen J, He H et al (2017) Cortical bone trajectory screws placement via pedicle or pedicle rib unit in the pediatric thoracic spine (T9–T12): a 2-dimensional multiplanar reconstruction study using computed tomography. *Medicine* 96:e5852
- Kim YJ, Lenke LG, Bridwell KH et al (2004) Free hand pedicle screw placement in the thoracic spine: is it safe? *Spine* 29:333–342
- Matsukawa K, Yato Y, Hynes RA et al (2017) Cortical bone trajectory for thoracic pedicle screws: a technical note. *Clin Spine Surg* 30:E497–E504
- Jendoubi K, Khadri Y, Bendjaballah M et al (2018) Effects of the insertion type and depth on the pedicle screw pullout strength: a finite element study. *Appl Bionics Biomech* 2018:1–9
- Huang J, Xie G, Liu Z (2008) FEA of hyperelastic rubber material based on Mooney-Rivlin model and Yeoh model. *China Rubber Ind* 8:22–26
- Kurutz M (2010) Finite element modelling of human lumbar spine. *Finite Element Analysis*. IntechOpen, London
- Kim YJ, Lenke LG (2005) Thoracic pedicle screw placement: free-hand technique. *Neurol India* 53:512
- Rancourt D, Shirazi-Adl A, Drouin G et al (1990) Friction properties of the interface between porous-surfaced metals and tibial cancellous bone. *J Biomed Mater Res* 24:1503–1519
- Bess S, Harris JE, Turner AW et al (2017) The effect of posterior polyester tethers on the biomechanics of proximal junctional kyphosis: a finite element analysis. *J Neurosurg Spine* 26:125–133. <https://doi.org/10.3171/2016.6.SPINE151477>
- Rodnoï P, Le H, Hiatt L et al (2021) Ligament Augmentation with mersilene tape reduces the rates of proximal junctional kyphosis and failure in adult spinal deformity. *Neurospine* 18:580–586. <https://doi.org/10.14245/ns.2142420.210>
- Safae MM, Deviren V, Dalle Ore C et al (2018) Ligament augmentation for prevention of proximal junctional kyphosis and proximal junctional failure in adult spinal deformity. *J Neurosurg Spine* 28:512–519. <https://doi.org/10.3171/2017.9.SPINE1710>
- Kim YJ, Bridwell KH, Lenke LG et al (2006) Pseudarthrosis in long adult spinal deformity instrumentation and fusion to the sacrum: prevalence and risk factor analysis of 144 cases. *Spine* 31:2329–2336
- Wilke H-J, Herkommer A, Werner K et al (2017) In vitro analysis of the segmental flexibility of the thoracic spine. *PLoS ONE* 12:e0177823
- Glattes RC, Bridwell KH, Lenke LG et al (2005) Proximal junctional kyphosis in adult spinal deformity following long instrumented posterior spinal fusion: incidence, outcomes, and risk factor analysis. *Spine* 30:1643–1649
- Helgeson MD, Shah SA, Newton PO et al (2010) Evaluation of proximal junctional kyphosis in adolescent idiopathic scoliosis following pedicle screw, hook, or hybrid instrumentation. *Spine* 35:177–181
- Tsutsui S, Hashizume H, Yukawa Y et al (2021) Optimal anchor at the uppermost instrumented vertebra in long fusion from the pelvis to the lower thoracic spine in elderly patients with degenerative spinal deformity: hook versus pedicle screw. *Clin Spine Surg* 35:E280–E284
- Ha Y, Maruo K, Racine L et al (2013) Proximal junctional kyphosis and clinical outcomes in adult spinal deformity surgery with fusion from the thoracic spine to the sacrum: a comparison of proximal and distal upper instrumented vertebrae. *J Neurosurg Spine* 19:360–369
- Cammarata M, Aubin C-É, Wang X et al (2014) Biomechanical numerical factors for proximal junctional kyphosis: a detailed numerical analysis of surgical instrumentation variables. *Spine* 39:E500–E507
- Yagi M, King AB, Boachie-Adjei O (2012) Incidence, risk factors, and natural course of proximal junctional kyphosis: surgical outcomes review of adult idiopathic scoliosis. Minimum 5 years of follow-up. *Spine* 37:1479–1489
- Wang H, Ding W, Ma L et al (2017) Prevention of proximal junctional kyphosis: are polyaxial pedicle screws superior to monoaxial pedicle screws at the upper instrumented vertebrae? *World Neurosurg* 101:405–415

26. Smith MW, Annis P, Lawrence BD et al (2015) Acute proximal junctional failure in patients with preoperative sagittal imbalance. *Spine J* 15:2142–2148

Publisher's Note Springer Nature remains neutral with regard to jurisdictional claims in published maps and institutional affiliations.

Authors and Affiliations

Edin Nevzati¹ · Manuel Moser¹ · Nick Dietz² · Burt Yaszay³ · Lawrence G. Lenke⁴ · Mazda Farshad⁵ · Varun Arvind⁶ · Samuel K. Cho⁶ · Alexander Spiessberger⁷ 

¹ Department of Neurosurgery, Cantonal Hospital Lucerne, Luzern, Switzerland

² Department of Neurosurgery, University of Louisville, Louisville, KY, USA

³ Department of Orthopedic Surgery, Rady's Children Hospital San Diego, San Diego, USA

⁴ Department of Orthopedic Surgery, Columbia University, New York, USA

⁵ Department of Orthopedics, Balgrist University Hospital, University of Zurich, Zurich, Switzerland

⁶ Department of Orthopedic Surgery, Icahn School of Medicine, Mount Sinai Hospital, New York, USA

⁷ Department of Neurosurgery, North Shore University Hospital, 300 Community Drive, Manhasset, NY 11030, USA